Design optimization of a tapered mirror for microfocusing optics

MAO Cheng-Wen(毛成文)   XI Zai-Jun(席再军)   YU Xiao-Han(余笑寒)[1)]   XIAO Ti-Qiao(肖体乔)

(Shanghai Synchrotron Radiation Facility, Shanghai Institute of Applied Physics, CAS, Shanghai 201800, China)

Abstract   A facile microfocusing optical design is presented which is optimized for less slope error against the traditional tapered mirror. The essential idea of the innovation is based on the characteristics of the slope-error curve for the prototype. The relationship between the mirror shape of the improved model and the driving moments is established. Analytical results have been compared with the results of the prototype. The design demonstrates theoretically that smaller slope error is obtained with longer active length.

Key words   microfocusing, dynamical bender, tapered mirror, slope error, shadow

PACS   42.15.Eq, 42.79.Fm

1   Introduction

With the recent availability of high-brilliance third-generation synchrotron sources, there is an immediate need for efficient X-ray microfocusing optics. Efforts are currently underway to produce microfocusing optics by a variety of means including tapered capillaries, Bragg-Fresnel optics, Fresnel Zone plates, compound refractive lenses and Kirkpatrick-Baez (KB) mirrors[1].

Dynamical bending devices for X-ray focusing optics in synchrotron radiation applications are getting more and more attractive. Such devices can be used to change the mirror surface shape easily to meet the focal distance variability requirement. Mechanical benders have mostly been used for this purpose. A cylindrical shape can be achieved by using a mechanical or a pneumatic bender with identical moments applied at the end of a rectangular mirror substrate[2]. The ideal mirror surface shape for point-to-point focusing is an ellipse. Elliptical bending X-ray mirrors can be produced by applying unequal moments to the two ends of a mirror of variable width or variable thickness. Two elliptical mirrors arranged in KB[1] geometry will be used as the microfocusing device for the hard X-ray microfocusing beamline at SSRF.

A major obstacle to the use of KB mirrors is the need to create elliptical surfaces with an X-ray quality figure and roughness. As a small focal spot is often required, it is more and more difficult to apply the moment or force with sufficient accuracy. The mirror with high precision of surface-shape, longer active length and lesser slope error, will meet the requirement well.

There are several methods to produce an elliptical mirror. Traditional elliptical benders employ a polynomial width mirror[2] substrate. And elliptical mirrors with bent-polishing methods[3] have also been fabricated for microfocusing by the KB configuration. As illustrated earlier, differential deposition[4] on the cylindrical substrate is also used to produce small monolithic elliptical mirrors for X-ray microfocusing. Since the mirror is shaped permanently, this approach is suitable for applications when the distance between the source and mirror is fixed, and less tolerant to manufacturing errors.

Another different bender employs a tapered mirror substrate[5]. A tapered substrate with a laterally-graded multilayer[6] is also used to produce an elliptical mirror. The manufacturing requirements of this mirror substrate are within the capabilities of current technology. The shape and slope error of the KB mirror could be controlled by two applied moments and a tapered angle.

This paper deals with the theoretical analysis of the improved model in terms of the tapered mirror characteristics. The improved design, based on the slope error curve of the prototype, is made to obtain lesser slope error and longer active length.

2 Principle and method of the new design

2.1 Tapered mirror

Ideally, the perfect ellipse surface shape can be represented by the following Eq.

$$z_e(x) = \frac{(p+q)\sin\theta}{4pq+(p-q)^2\cos^2\theta} \times$$

$$\left\{2pq - 2[(pq)^2 - pqx^2 - xpq(p-q)\cos\theta]^{1/2} - \right.$$

$$x\cos\theta(p-q)\} \tag{1}$$

or by a high order polynomial[2]

$$z_e(x) = \sum_{i=2}^{\infty} a_i x^i, \tag{2}$$

where z_e is the surface height of an ideal ellipse mirror, x is the coordinate along the mirror surface and its origin is on the mirror centre, p and q are the source and image distance, respectively and θ is the grazing incident angle (Fig. 1). The coefficients a_i[2] are
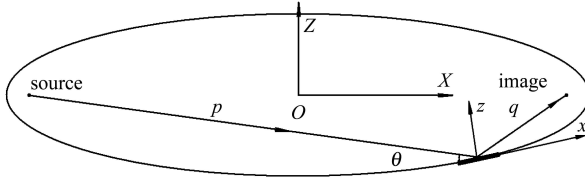

Fig. 1. Working condition and coordinate definition of the elliptical focusing mirror.

$$a_2 = \frac{1}{4}\frac{(p+q)}{pq}\sin\theta,$$

$$a_3 = \frac{a_2}{2}\left(\frac{1}{q} - \frac{1}{p}\right)\cos\theta,$$

$$a_4 = \frac{1}{16}a_2\left[\frac{4}{pq} + 5\left(\frac{1}{q} - \frac{1}{p}\right)^2\cos^2\theta\right],$$

$$a_5 = \frac{1}{32}a_2\cos\theta\left(\frac{1}{q} - \frac{1}{p}\right) \times$$

$$\left[\frac{12}{pq} + 7\left(\frac{1}{q} - \frac{1}{p}\right)^2\cos^2\theta\right]\cdots. \tag{3}$$

Approximating the mirror as a beam, the bending of the mirror fits in with standard mechanical beam theory. The shape of the actual mirror surface under the action of two different moments M_1 and M_2 is defined

by the following Eq.[7, 8]

$$EI\frac{d^2z_r}{dx^2} = \frac{M_1+M_2}{2} + \frac{M_2-M_1}{L}x, \tag{4}$$

where z_r is the surface height of the actual mirror, E is Young's modulus of the mirror substrate material, I is the moment of inertia of the rectangular beam cross section ($I = bt^3/12$, b and t are the width and thickness of the mirror) and L is the distance between the two moments being applied.

The tapered mirror can also be viewed as a truncated triangle (Fig. 2). This mirror width can be defined by Eq.[5, 9]

$$b(x) = b_0(1+kx), \tag{5}$$

where b_0 is the width at the mirror centre, k is a constant correlated only with p, q and θ.

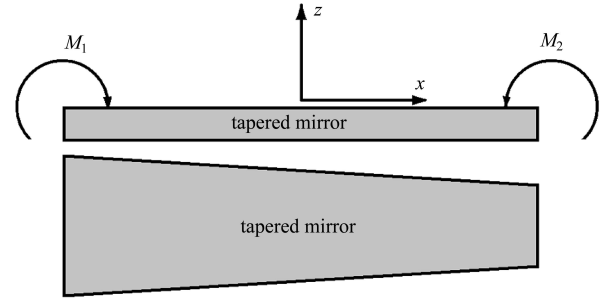

Fig. 2. The side view and top view of the tapered mirror.

Following the idea of Padmore et al.[7, 8], the expression for the moments needed to produce the ellipse shape is[7]

$$\begin{aligned} M_1 &= EI_0(2a_2 - 3a_3L + 2a_2a_4L/a_3), \\ M_2 &= EI_0(2a_2 + 3a_3L - 2a_2a_4L/a_3). \end{aligned} \tag{6}$$

The constants k, c, d are defined as

$$k = -2a_4/a_3, \quad c = 2a_2,$$

$$d = 6a_3 - \frac{4a_2a_4}{a_3}. \tag{7}$$

So, the shape of the actual mirror surface $z_r(x)$ is the following Eq.[5]

$$\frac{d^2z_r}{dx^2} = \frac{c+dx}{1+kx} \tag{8}$$

or is represented by another Eq.[5]

$$z_r = \frac{d}{2k}x^2 + \frac{ck-d}{k^3}(1+kx) \times$$

$$\left[\ln(1+kx) - 1\right] + \frac{ck-d}{k^3}. \tag{9}$$

It is shown (Fig. 3) that all values of the curve of slope error are positive except the zero value at the mirror centre. For a smaller microfocusing spot and

high brightness, lesser slope error and longer active length are absolutely necessary. It is obviously noted (Fig. 3) that the active length is only several centimeters with the value of the slope error below 0.1 μrad.
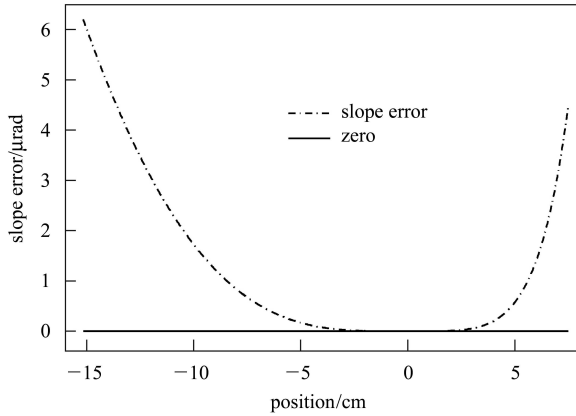

Fig. 3. Slope error of the tapered mirror (p=5 m, q=0.2 m, θ=4 mrad, $k = -2a_4/a_3 = -6.2 \times 10^{-2}$).

2.2 Improved model of the tapered mirror

From Fig. 3, the value of the slope error curve except at the centre is positive, and there is only a short active length of the prototype which accords well with the rigorous requirements on the precision of the mirror surface at the microfocusing beamline. Based on the characteristics of the slope error curve of the original tapered mirror, the value of the slope error can be minimized by an improved model of the tapered mirror in which the constant k is variable at the right point on the mirror (shown by Fig. 4). The top view of the new design looks like a combination of several tapered parts. The middle part of the new design accords with the original model.
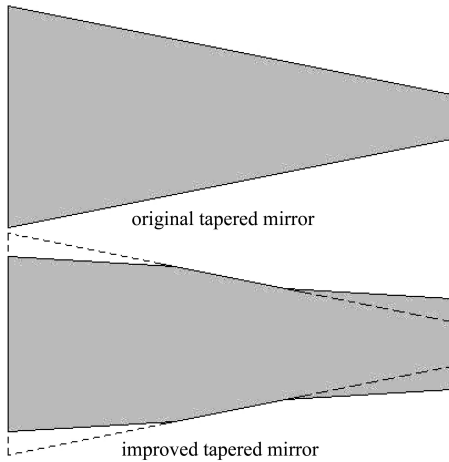

Fig. 4. The top view of the improved tapered mirror model.

The width of the new mirror can be defined by Eq.

$$\frac{b(x)}{b_0} = \begin{cases} (1-\Delta k_1 x_A)+(k+\Delta k_1)x & x \leqslant x_A < 0 \\ (1+kx) & x_A < x < x_B \\ (1-\Delta k_2 x_B)+(k+\Delta k_2)x & 0 < x_B \leqslant x \end{cases} \tag{10}$$

where x_A $(x_A < 0)$ and x_B $(x_B > 0)$ are the inflexions at two sides of the mirror.

The shape of the new design part $(x < x_A < 0$ or $x > x_B > 0)$ is the following Eq.

$$z''_\Delta = \frac{d}{k+\Delta k_1} + \frac{c(k+\Delta k_1)-d(1-\Delta k_1 x_A)}{k+\Delta k_1} \times \frac{1}{(1-\Delta k_1 x_A)+(k+\Delta k_1)x}, \tag{11}$$

or by the following Eq.

$$z_\Delta = \varphi x + \frac{d}{2(k+\Delta k_1)}x^2 + \frac{c(k+\Delta k_1)-d(1-\Delta k_1 x_A)}{(k+\Delta k_1)^3} \times \left\{ \ln[(1-\Delta k_1 \cdot x_A)+(k+\Delta k_1)x]-1 \right\} \times [(1-\Delta k_1 \cdot x_A)+(k+\Delta k_1)x] + \phi, \tag{12}$$

where φ and ϕ are two coefficients:

$$\varphi = \left(\frac{d}{k} - \frac{d}{k+\Delta k_1}\right)x_A + \left[\frac{ck-d}{k^2} - \frac{c(k+\Delta k_1)-d(1-\Delta k_1 x_A)}{(k+\Delta k_1)^2}\right]\ln(1+kx_A),$$

$$\phi = -\varphi x_A + \frac{1}{2}\left(\frac{d}{k}-\frac{d}{k+\Delta k_1}\right)x_A^2 + \left[\frac{ck-d}{k^3} - \frac{c(k+\Delta k_1)-d(1-\Delta k_1 x_A)}{(k+\Delta k_1)^3}\right] \times [\ln(1+kx_A)-1]\cdot(1+kx_A) + \frac{ck-d}{k^3}.$$
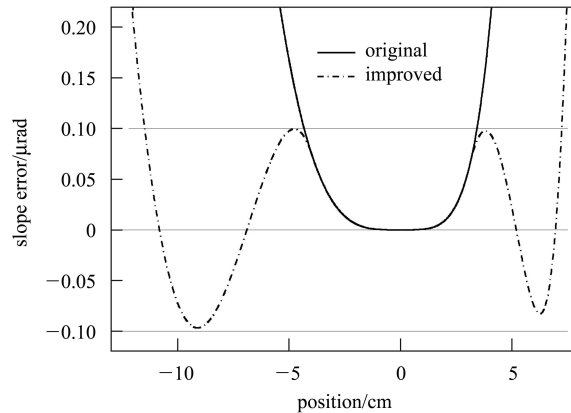

Fig. 5. The slope errors of the improved tapered mirror and the original model in the configuration of p=5 m, q=0.2 m, θ=4 mrad, $k = -6.2 \times 10^{-2}$, $x_A = -3.9876$ cm, $\Delta k_1 = 2.28\times10^{-3}$, $x_B = 3.1346$ cm, $\Delta k_2 = 1.54\times10^{-3}$.

It is shown (Fig. 5) that the active length, with the slope error value below 0.1 μrad, approaches 20 cm which compares intensively with the prototype.

2.3 The results from the software shadow

The mirrors are in the configuration of p=500 cm, $q = 20$ cm, $\theta = 4$ mrad, the lengths of the mirrors are 18 cm. The spot sizes of microfocusing of the original tapered mirror and the new design are calculated by a software shadow (Fig. 6). The spot size of the microfocusing of the perfect ellipse shape is calculated by the software shadow (Fig. 7).
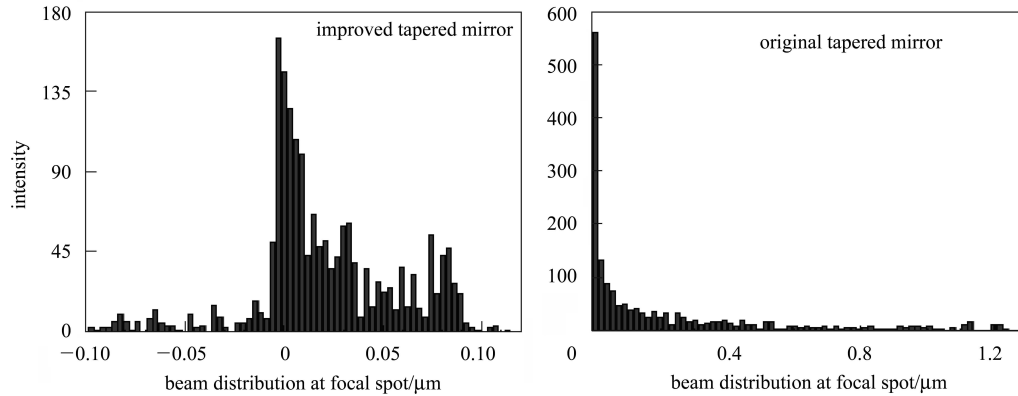

Fig. 6. The beam distribution at the focal spot of the improved tapered model and original mirror in the configuration of $p = 500$ cm, $q = 20$ cm, the grazing incident angle $\theta = 4$ mrad, and the length of the mirror is almost 18 cm.
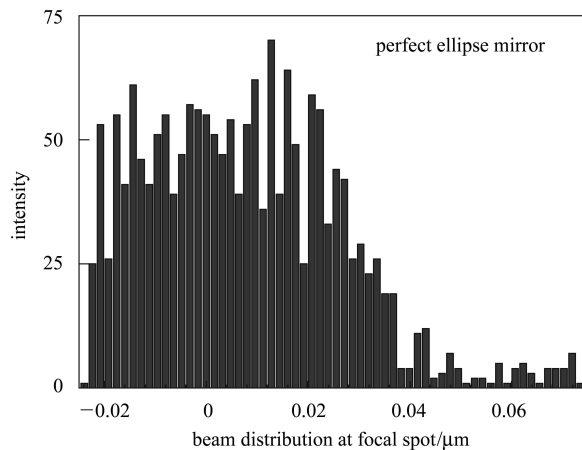

Fig. 7. The beam distribution at the focal spot of the perfect ellipse mirror.

It is shown (Fig. 6 and Fig. 7) that the smaller focusing spot which is close to the result of the perfect ellipse is obtained with the improved tapered mirror, compared enormously with the original tapered mirror. It is deduced that the new design of the tapered mirror meets suitably the rigorous requirements of microfocusing.

3 Conclusions

A theoretical analysis and parameters study of the improved design of the tapered mirror have been presented. The relationship between the mirror shape of the improved model and the driving moments is established. Analytical results have been compared with the results of the prototype. The design demonstrates theoretically that, by changing the constant k suitable at the right place on the mirror, smaller slope error is obtained with longer active length. The manufacturing requirements of the improved mirror substrate are within the capabilities of current technology like the traditional tapered mirror.

References

1 YANG B X, Rivers Mark, Schildkamp Wilfried, Eng P J. J. Synchrotron Rad., 1995, **2**: 2278
2 Eng P J, Rivers M L, YANG B X et al. Proc. SPIE, 1995, **2516**: 41
3 Kirkpatrick P, Baez A. J. Opt. Soc. Am, 1948, **38**: 766
4 Underwood J H. Space Sci. Instr., 1997, **3**: 259
5 Takeuchi Akishisa, Suzuki Yoshio, Takano Hidekazu, Yasuko Terada. Rev. Sci. Instr., 2005, **76**: 093708
6 Ice G E, Chung Jin-Seok, Tischler J Z. Rev. Sci. Instr., 2000, **71**(N7): 2635—2639
7 Ziegler E, Hignette O, Morawe Ch, Tucoulou R. Nucl. Instrum. Methods Phy. Rea. A, 2001, **954**: 467
8 Padmore H A, Hawells M R, Irick M R, Renner T, Sandler R, Koo Y-M. Proc. SPIE, 1996, **2856**: 145
9 Howells M R, Cambie Daniela, Duarte R M et al. Opt. Eng., **39**(10): 2748